IEEE Access
Multidisciplinary ⋮ Rapid Review ⋮ Open Access Journal

Received 8 June 2023, accepted 18 June 2023, date of publication 23 June 2023, date of current version 3 July 2023.

*Digital Object Identifier 10.1109/ACCESS.2023.3289004*

RESEARCH ARTICLE

# An Electromagnetic-Piezoelectric Hybrid Harvester Based on Magnetic Circuit Switch for Vibration Energy Harvesting

**XIANG GAO[1,2], JUAN CUI[1,3], YONGQIU ZHENG[1], GANG LI[1], CONGCONG HAO[1], AND CHENYANG XUE[1]**

[1]Key Laboratory of Instrumentation Science and Dynamic Measurement, Ministry of Education, North University of China, Taiyuan 030051, China
[2]Department of Mechanics, Jinzhong University, Jinzhong 030619, China
[3]State Key Laboratory for Manufacturing Systems Engineering, Xi'an Jiaotong University, Xi'an 710049, China

Corresponding author: Juan Cui (cuijuan@nuc.edu.cn)

This work was supported in part by the National Key Research and Development Program of China under Grant 2019YFB2004800, and in part by the Fundamental Research Program of Shanxi Province under Grant 20210302124033 and Grant 202102100401014.

**ABSTRACT** Energy harvesting technologies are contributing to the development of the Internet of Things. These techniques can provide continuous, energy-efficient and environmentally friendly power supplies and reduce manual maintenance requirements, and thus have strong prospects for sensing and monitoring applications, particularly in certain harsh working environments. The proposed electromagnetic–piezoelectric hybrid harvester contains both electromagnetic generator (EMG) and piezoelectric generator (PEG). Through vibration of the cantilever beam, the magnetic circuit in the soft-magnetic material is both connected and disconnected, and this can cause the magnetic flux in the coil to change dramatically, resulting in induction of a large voltage in the coil. This paper illustrates the feasibility and the optimal characteristics of the proposed hybrid harvester using theoretical verification and simulations, and demonstrates the factors that affect the power generation effect through testing. The study found that the maximum open-circuit voltages of the EMG and the PEG are 16 V and 42 V and the maximum peak powers of the EMG and the PEG reach 20 mW and 35 mW, respectively. The proposed energy harvester offers advantages in terms of both peak voltage and peak power, and provides a new method and concept for the vibration energy harvesting field.

**INDEX TERMS** Energy harvesting, magnetic circuit switch, cantilever beam, magnetic flux.

## I. INTRODUCTION

The Internet of Things (IoT) and wireless sensor networks (WSNs) are used widely in industrial production. Sensor nodes that are distributed in key parts of the industrial device can collect signals effectively to determine the running status of that device [1], [2], [3], [4]. However, supplying power to the numerous nodes required represents a major issue because regular replacement or recharging of their batteries can incur heavy manual maintenance costs, while use of cabled power supplies can cause frequent failures [5]. A vibration energy harvester can capture vibration energy generated during the operation of large-scale equipment and use this energy to power the sensing nodes in critical parts of the equipment, thus effectively avoiding the aforementioned power supply problems [6], [7], [8]. In recent years, increasing attention has been paid to energy harvesting techniques for industrial equipment because of its great application prospects. This approach is particularly suitable for certain special working environments, including coal mines and other harsh application environments, to ensure the safety of the personnel.

The available methods that can convert mechanical energy into electrical energy efficiently include electromagnetic [9], [10], [11], [12], [13], [14], [15], piezoelectric [16], [17], [18], [19], [20], [21] and triboelectricity-based methods [22], [23], [24], [25], [26]. Sometimes, depending on the structural characteristics of the energy harvester, these energy harvesting techniques can be integrated to achieve a better overall

The associate editor coordinating the review of this manuscript and approving it for publication was Tao Wang.

power generation effect. Among these methods, electromagnetic energy harvesting is commonly used in vibration energy harvesting because it offers comparatively higher power generation [27]. Of the existing electromagnetic energy harvester configurations, the tube structure has been studied by many researchers. In this structure, a voltage is induced in a coil wound around the cylinder wall by magnets vibrating up and down inside the cylinder. Yang et al. studied a magnetic levitation-type electromagnetic energy collector that achieved tri-stable states by adding four small magnets at the center of the cylinder. The main advantage of this structure is that it broadens the operating frequency band of the generator. Under the conditions of 1g and 8Hz, a peak power output of 6.9mW can be achieved. Its working frequency band is 3-8Hz [28]. Zhang et al. used three cylindrical magnets to levitate the circular main magnet that enabled energy harvesting in the case of micro-vibrations. Under the conditions of 1g and 6Hz, The peak power of electromagnetic power generation is 1.6mW [29]. Iqbal et al. introduced a spiral planar spring to extend the operating frequency band of a permanent magnet during vibrations [10], [30]. Under the conditions of 0.6g and 9.7Hz, the peak power of electromagnetic power generation is 0.18mW. The operating frequency of these structures is concentrated at around 10 Hz and thus they are only suitable for low-frequency vibration environments. The output performances of these structures are greatly reduced in working environments with operating frequencies above 20 Hz. In addition, electromagnetic energy harvesters can have many different structures [31]. For example, Gu et al. designed a cup-shaped harvester structure. Vibrations in any direction caused the magnetic sphere inside this structure to shift, causing the surrounding coils to induce a voltage. Under the conditions of 1g and 5Hz, the peak power of electromagnetic power generation is 0.13mW [32]. These different design forms offer certain advantages in terms of broadening the frequency band and the energy harvesting direction, but their operating frequencies are still low and they cannot be used widely in vibrating equipment.

One effective way to increase the working frequency is to use a cantilever beam structure [33]. A coil or magnet located on the beam is driven to move up and down by the vibration of the beam, the magnetic flux then varies with the relative displacement of the coil and the magnet and an induced voltage is generated. This method can be combined with a piezoelectric energy harvester to improve the power generation performance. Burrow et al. studied a structure with a magnet located at the end of a cantilever beam that could form a magnetic loop with the armature on a stator coil to provide effective power generation [34]. Abu Raihan Mohammad Siddique et al. designed a spring pull magnet structure at the end of a cantilever beam. Vibration of the cantilever beam drives the spring and the permanent magnet to move up and down and thus cause a coil situated near the permanent magnet to generate an induced voltage. Under the conditions of 0.8g and 7Hz, the peak power of electromagnetic power generation is 0.22mW [35]. In these methods, the cantilever beam is used as the traction component to cause the permanent magnet to shift. The end load of the cantilever beam is generally fixed, which means that the overall tunability of the structure deteriorates and it cannot be adapted to different types of vibrating equipment.

It can be concluded from the descriptions of the electromagnetic energy harvester devices above that their energy harvesting mode involves changing the magnetic flux in a coil through relative displacement of a permanent magnet and a coil. This type of energy harvesting method relies on movement of either the coil or the magnet to produce electricity. The magnetic flux changes slowly and the peak voltages are usually low, which means that this approach is not suitable for matching with different vibrating equipment types. Herein, an electromagnetic-piezoelectric hybrid energy harvester combined with a magnetic circuit switch (MCS) based on the cantilever beam structure is proposed. The change in magnetic flux does not require relative displacement of the coil and the magnet, but relies on the change in the clearance between the cantilever beam and the coil column that is caused by vibration. In addition, a piezoelectric energy harvester is added to the cantilever beam to collect vibration energy and thus improve the power generation efficiency of the device. This energy harvesting scheme can improve both the peak voltage and the instantaneous power effectively. Furthermore, the frequency band of the harvester can be changed by simply adjusting the cantilever beam to adapt to different vibration environments. We tested the cantilever beam with different thicknesses and determined that the cantilever beam thickness would affect the operating frequency of the hybrid energy harvester, but has little effect on output voltage. The test results are shown in supplementary material Figure S1.

## II. STRUCTURE AND THEORETICAL ANALYSIS

The structure and materials of the proposed electromagnetic–piezoelectric hybrid harvester is shown in Figure 1(a) and 1(b). The upper and lower ends of the columnar permanent magnet are connected to a cantilever beam and a bottom plate, respectively. The distal end of the bottom plate is connected to a coil column via a screw thread, and the position of this coil column can be adjusted using different threads. Commercially available Pb(Zr1−xTix)O3 ( PZT ) was used as the piezoelectric material. The PZT is placed at the clamped end of the cantilever beam, and a mass is pasted on the free end of the cantilever beam. The coil column, the cantilever beam, and the bottom plate are all made from spring steel (55SiCr63) because of its good magnetic conductivity. The yield strength and the fatigue limit of this material are also high. When the cantilever beam is in contact with the coil column, these three components form a magnetic circuit together with the permanent magnet. This magnetic circuit is much more conductive than the surrounding air, which means that most of the magnetic flux is concentrated within the magnetic circuit. When the cantilever is disconnected from

the coil column, the magnetic flux in the magnetic circuit is reduced, and some of the magnetic flux is then carried through the air.

The designed hybrid energy harvester includes two power generation methods, namely piezoelectric generator (PEG) and electromagnetic generator (EMG). The working principle of the (PEG) is described as shown in Figure 1(c). The PZT is stuck near the fixed end of the beam, it presents a periodic contraction and tension state with the vibration of the beam, and the electrical energy is generated owing to the d31 piezoelectric effect, the charge is distributed at the upper and lower of the PZT. The distribution of charges changes with contraction and tension to produce opposite polarities, resulting in opposite currents. Figure 1(d) shows the principle of the electromagnetic energy harvester simulated by COMSOL software. It illustrates the distributions of the magnetic flux density when the cantilever beam makes contact and separates from the coil column. As can be seen from the figure, there is a very significant change in the flux density inside the coil column for two states. During the vibration of the cantilever beam, the flux density in the coil column is low when the beam is separated from the coil column, and increases sharply when the beam is in contact with the coil column. Figure 1(e) shows the distribution of magnetic induction lines and the direction of current in the coil when the beam is in different positions. In the initial state, the magnet and the magnetic conductive material do not form a complete path, so a part of the magnetic inductance line passes through the air, and there is no induction current in the coil of the electromagnetic generating unit. When the cantilever beam moves downward to contact with the coil column under the action of external vibration energy, the permanent magnet and the soft magnetic material form a closed path, most of the magnetic inductance line is concentrated in this magnetic circuit, so that the magnetic flux in the coil column increases rapidly, resulting in a larger voltage induced in the coil. Under the stress, the cantilever beam starts moving upward from the lowest point. At the instant when the cantilever beam is separated from the coil column, the path described above is disconnected. The magnetic flux in the coil column decreases rapidly as a result, and a large reverse voltage is induced in the coil. After separation, the cantilever beam continues to move upward, and then the flux decreases slightly until the cantilever beam reaches its maximum upward displacement. At this point, the magnetic inductance line in the coil decreases to a minimum, the leakage in the air reaches a maximum, and the direction of the current in the coil remains unchanged. The cantilever then begins to move downward, the magnetic induction lines in the coil column slowly increase, and the direction of the current generated in the coil changes until the cantilever beam is in contact with the coil column to form a complete circuit in which the magnetic induction lines are overwhelmingly concentrated.

In order to describe the power generation performance of electromagnetic - piezoelectric hybrid harvester theoretically, we model the hybrid harvester. The system motion is usually

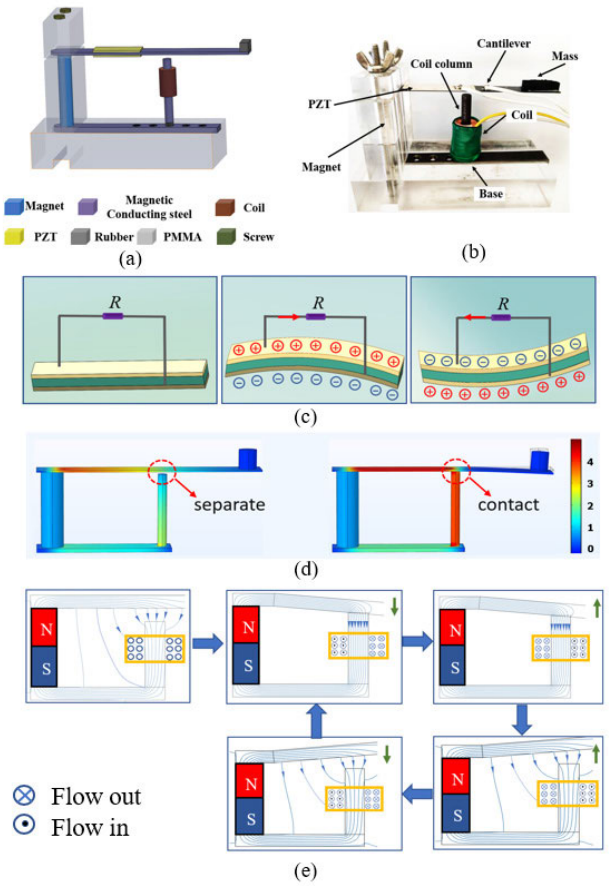


**FIGURE 1.** (a) Structure design of the hybrid harvester. (b) Photograph of the hybrid harvester and labels of each component. (c) The working mechanism of the PEG. (d) COMSOL simulation of magnetic flux density under two states of contact and separation. (e) The working principles of the EMG.

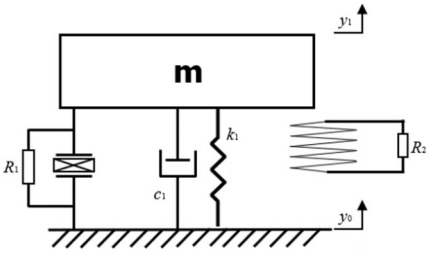


**FIGURE 2.** Lumped parameter model.

equivalent to the spring, mass and damping. The lumped parameter model [34], [36] was constructed as shown in Figure 2. Let $y = y_1 - y_0$, and the motion equation of the harvester is given by

$$m\ddot{y} + c\dot{y} + ky + F_p + F_e = 0 \tag{1}$$

where $m$ is the end mass of the beam, $c$ is the equivalent damping of the beam, $k$ is the equivalent stiffness of the beam. In addition to the cantilever force, the vibration system also has the reaction force generated by piezoelectric and electromagnetic unit. $F_p$ is the reaction force of the piezoelectric

unit, $F_e$ is the reaction force of the electromagnetic unit. Reaction force of the piezoelectric $F_p$ can be derived from the following formula

$$F_p = \Theta_p v_{R1} \tag{2}$$

where $\Theta_p$ is proportional to the piezoelectric constant (d31) of the piezoelectric patch. $V_{R1}$ is the Voltage across the external resistance (R1) of the piezoelectric patch. According to Kirchhoff's current law, the equation for the piezoelectric unit is

$$\Theta_p y - \frac{v_{R1}}{R1} = C_p \dot{v}_{R1} \tag{3}$$

Reaction force of the electromagnetic unit $F_e$ can be derived from the following formula

$$F_e = \Theta_e I_e \tag{4}$$

where $\Theta_e$ is the electromechanical coupling coefficient, $I_e$ is the induced current of electromagnetic unit.

The equation for the electromagnetic unit is

$$-\Theta_e \dot{y} + L_c \dot{I}_e + (R_c + R_2) I_e = 0 \tag{5}$$

in which $L_c$ is the inductance of the coil, $R_c$ is the coil resistance, $R_2$ is the external resistance connected to the coil.

The overall dynamic equations of the harvester can then be expressed as

$$\begin{cases} m\ddot{y} + c\dot{y} + ky + F_p + F_e = 0 \\ \Theta_p y - \frac{v_{R1}}{R1} = C_p \dot{v}_{R1} \\ -\Theta_e \dot{y} + L_c \dot{I}_e + (R_c + R_2) I_e = 0 \end{cases} \tag{6}$$

## III. EXPERIMENTS AND RESULTS

To obtain the output performance of the device, a test platform was built to perform experimental research. As shown in Figure 3, the target spectrum signal was set up in computer software and then transmitted to the controller (ECON VT -9008), which generates the shaker motion control signal and also controls the shaker (ECON VE-5120ST) vibration after amplification by the amplifier(ECON VSA-H751A). This approach enables precise control of the shaker's operating vibration acceleration and the vibration amplitude. The output voltage of electromagnetic unit and piezoelectric unit are measured by a digital storage oscilloscope (GWINSTEK GDS-3504), and the output power is measured by the power analyzer (ZLG PA5001H). The energy harvester is fixed to the shaker and is used to collect the vibration energy. Different energy harvester component materials and sizes have a major impact on its output performance. The parameters used in the fabrication of each component of the energy harvester are listed in Table 1.

According to the different contact conditions existing between the cantilever beam and the coil column during the vibration process, it can be divided into three different operating states, i.e. contact and separation mode, non-contact mode and continuous contact mode. Figure 4(a) shows the schematic diagram of the contact and separation mode and the output curves of the electromagnetic generation units and piezoelectric generation units. The contact and separation mode is where the cantilever beam is able to make contact with the coil column as it vibrates downward and is able to move upward at that point due to the stress being greater than the magnetic suction. According to the previous description of the operating principle, there is a very sharp change in the magnetic flux in the coil during the time between the contact and separation of the cantilever beam and the coil column, so that the EMG unit generates a spike voltage. As can be seen from the waveform of EMG, a peak high voltage is generated because there is a very dramatic change in the magnetic flux in the coil during the contact and separation time between the cantilever and the coil column as described above in the principle of operation. The PEG unit has its original sinusoidal waveform somewhat altered due to the blocking of the coil column. Figure 4(b) presents the schematic diagram of the continuous contact mode and the output curves of the EMG units and PEG units. The continuous contact mode is one in which the stress on the cantilever beam is not sufficient to overcome the magnetic suction, resulting in a continuous contact between the beam and the coil post. In this mode, both EMG units and PEG units are unable to perform effective voltage output. Figure 4(c) depicts the non-contact mode of operation and the waveforms of ENG and PEG in this mode of operation. The non-contact mode is the case where the cantilever beam is not in contact with the coil column during the vibration. The waveform diagram of electromagnetic generation shows only a weak near-sine waveform. This is because the magnetic material does not form a closed loop and most of the magnetic flux is present in the air while only a small portion of the magnetic material is present, so the induced voltage generated during vibration is small. In this mode, PEG can output voltage normally because the vibration of the cantilever beam is not limited.

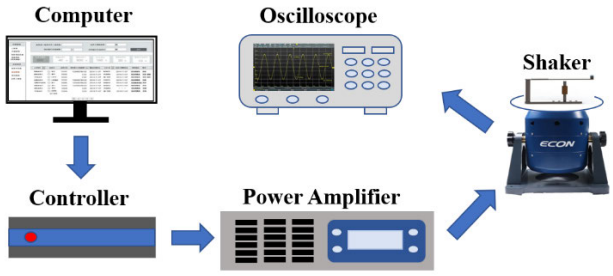


**FIGURE 3.** Experimental equipment of the hybrid energy harvester.

Performance tests were conducted with respect to the energy harvester's output, initially by testing its open - circuit voltage values relative to different frequencies and different accelerations. To characterize the output performance of each unit, we tested their open circuit peak voltages in the frequency range from 20 – 40 Hz under various excitation conditions (0.5 g, 1 g, 1.5 g and 2 g), with results as shown in Figure 5. When the acceleration is 0.5 g, the device is

**TABLE 1. Symbols and parameters.**

| Parameters | Values |
|---|---|
| Size of the cantilever beam | 100×10×0.4 (mm) |
| End mass (m1) | 10g |
| Size of the magnet | Φ6×40 (mm) |
| Size of the PZT | 30×10×0.2 (mm) |
| Coil number (n) | 1000 |
| Inner resistance of the coil | 173Ω |

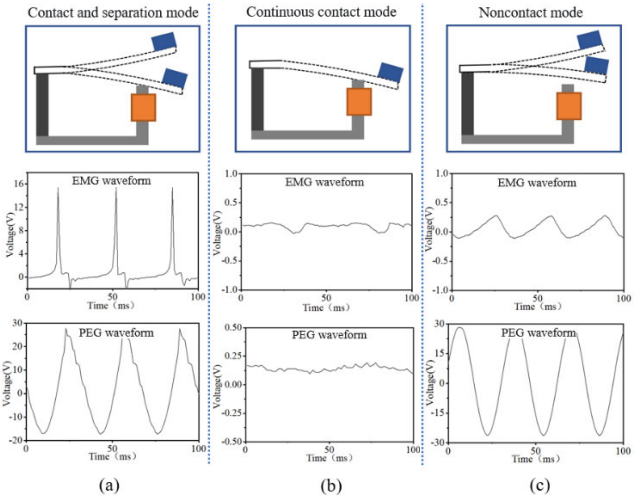


**FIGURE 4. Schematic diagram and Voltage waveforms for the EMG and the PEG in three modes. (a) Contact separation mode. (b) Continuous contact mode. (c) Non-contact mode.**

in noncontact mode. The cantilever beam vibrates normally and the piezoelectric energy harvester can output energy normally. Because the conductive material cannot form a closed loop, the electromagnetic output from the harvester is weak. When the acceleration is above 0.5 g, the device is in contact separation mode. The results show that both the electromagnetic and piezoelectric output voltages reach their maxima at 30 Hz, where the maximum output voltages obtained under 2 g acceleration are 16 V and 42 V, respectively. In addition, when the acceleration increases, the working band will then be broadened to a certain extent.

Based on the working principle of the device, the gap between the coil column and the cantilever beam is a highly important parameter. The distance of the gap is represented by d in the Figure 6. The output voltage characteristics of the EMG and the PEG at a frequency of 30 Hz and at accelerations of 2 g are shown in Figure 6 for gap sizes of 0.5 mm, 1 mm, 1.5 mm and 2 mm. Almost no voltages are output by the EMG and the PEG when the gap is 0.5 mm. The device is in continuous contact mode in this case. When the gap size is 1 mm, 1.5 mm and 2 mm, the peak open-circuit voltages of the electromagnetic unit are 7 V, 12 V and 16 V and the peak open-circuit voltages of the piezoelectric unit are 27 V, 35 V and 42 V, respectively. The device operates in contact separation mode in these three cases. The results show that the gap length has a linear relationship with the peak open-circuit voltage in this mode.

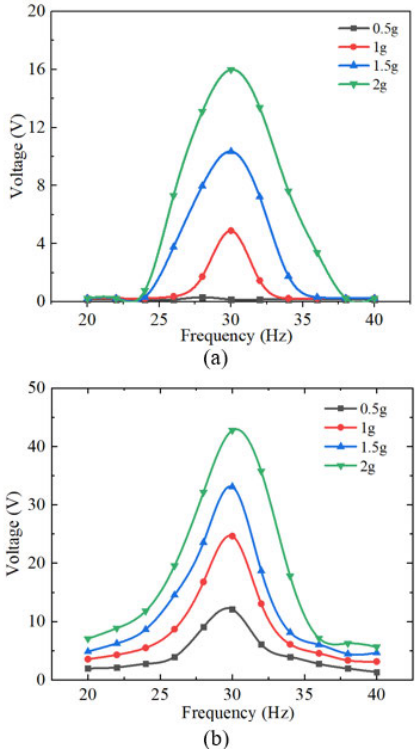


**FIGURE 5. Open circuit voltage with different frequencies and accelerations. (a) EMG. (b) PEG.**

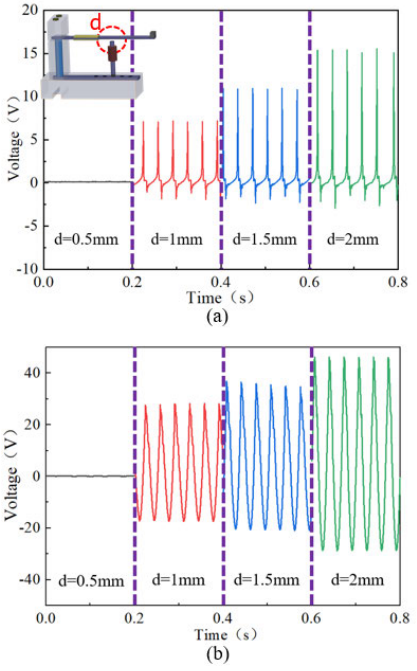


**FIGURE 6. Open circuit voltage with different gaps. (a) EMG. (b) PEG.**

The distance of the magnetic path between the permanent magnet and the permeable material also has a major impact

on the device output voltage. Here, we varied the distance of the magnetic path by changing the distance between the coil column and the permanent magnet. The distance between the coil column and the permanent magnet is represented by L in the Figure 7. The output voltage characteristics of the EMG and the PEG at a frequency of 30 Hz and acceleration of 2 g are shown in Figure 7 for L of 40 mm, 50 mm, 60 mm and 70 mm. The corresponding peak open-circuit voltages of the EMG and the PEG are 0.3 V, 16 V, 12 V and 4 V, and 32 V, 34 V, 30 V and 20 V, respectively.

When the distance is 40 mm, the EMG only shows a weak output voltage, while the output from the PEG is normal, which indicates that the device is working in the noncontact mode in this case. When the distance reaches 50 mm, the device operates in the contact separation mode. At this time, the peak open-circuit voltages of both the electromagnetic and piezoelectric units reach their maximum values. Thereafter, the peak open-circuit voltage decreases gradually. The EMG works best at the distance of 50 mm, indicating that a shorter path is better in contact separation mode. The PEG works best at the distance of 50 mm because of the finite effect of the coil column. As the distance away from the permanent magnet increases, the deformation of the cantilever beam decreases in tandem. The output open-circuit voltage thus tends to decrease in this scenario.

Connecting the EMG unit and PEG unit to the load resistor respectively, we can get its output voltage and power. According to the maximum power transfer theorem, it is known that the maximum output power can be obtained when the external load and the power load are the same. The internal resistance of the EMG unit and PEG unit can be measured to be 1.3k Ω and 19k Ω respectively through a multimeter. The impedance of the EMG unit and PEG unit have inductance and capacitance in addition to resistance, so the total impedance is higher than 1.3k Ω and 19k Ω. As can be seen in Figure 8, the EMG unit achieved maximum power at 3k, while the PEG achieved maximum power at 30k, which were 20 mW and 35 mW, respectively. At this time, the voltage on the load resistor was 5.3V and 23V, respectively. The voltage increases with the increase of load resistance value, and the maximum output voltage of EMG and PEG can reach 10V and 40V, respectively, when the resistance is 10k Ω and 100k Ω.

Table 2 shows a comparison of four typical piezoelectric and electromagnetic hybrid power generation works with this work. It can be seen that the working conditions of Zhou, Wang, and Tian's hybrid generators are all low-frequency and cannot be applied to mechanical vibration equipment. Only Zhang's hybrid generator has a working frequency of 20Hz, but its working acceleration reaches 39.2ms, requiring intense vibration energy to operate, much higher than the 14.7ms required for this operation. Among these four hybrid generators, the maximum output voltage and power of electromagnetic power generation are only 3V and 8mW, far lower than the operating 16V and 20mW. Therefore, the hybrid generator of this work is more suitable for energy harvest of mechanical vibration equipment than these four works, and electromagnetic power generation has better energy harvest effect.

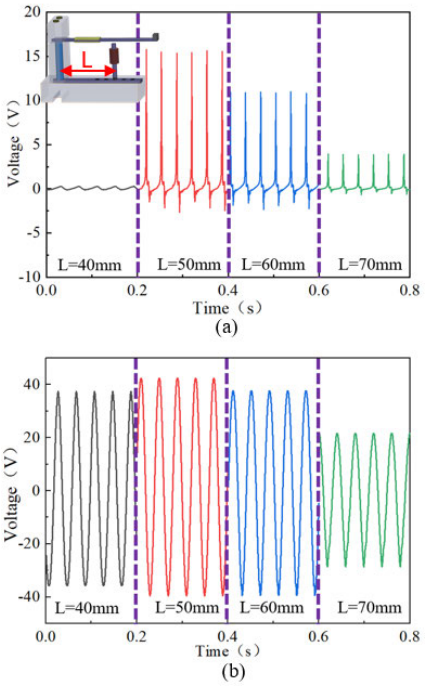


**FIGURE 7.** Open circuit voltage with different distance between the coil column and the permanent magnet. (a) EMG. (b) PEG.

To demonstrate that these hybrid harvesters can be used as sustainable power sources, three sets of practical demonstrations were performed in the laboratory. As shown in Figure 9(a), the electromagnetic unit output and the piezoelectric unit output from the energy harvester passed through their respective bridge rectifier circuits, and then the two outputs were connected in parallel to a thermometer, 50 LED lights and a capacitor. Figure 9(b) depicts a demonstration scenario in which the hybrid energy harvester powers a thermometer. Hybrid energy harvester collects the vibration energy from the shaker and converts it into electric energy, which is processed by the conditioning circuit to power the thermometer. When connected to the load composed of the LED lights, the lights can all be seen clearly to be lit in a dark environment, as shown in Figure 9(c). Figure 9(d) shows the characteristics of a 100 $\mu$F capacitor being charged by the individual units (electromagnetic, piezoelectric) and by the hybrid harvester. The voltage obtained within a charging time of 10 s was 6.9 V for the hybrid harvester, but only 5 V was realized when using the electromagnetic generator alone. The hybrid harvester thus offers a significant advantage in terms of its charging rate. Additionally, the saturation voltage was also higher for the electromagnetic–piezoelectric hybrid harvester. Three different capacitors were charged

**TABLE 2.** Comparison between previous works and this work.

| Reference | Transduction | Frequency, acceleration, internal resistance | Voltage, power |
|---|---|---|---|
| Zhou et al.(2022) [37] | Electromagnetic | 5Hz, 31.4m/s$^2$, 10kΩ | 2.6V, 0.2mW |
| | Piezoelectric | 5Hz, 31.4m/s$^2$, 10kΩ | 17V, 11mW |
| Wang et al.(2019) [38] | Electromagnetic | 5Hz, 9.8m/s$^2$, 0.3kΩ | 2.4V, 8mW |
| | Piezoelectric | 5Hz, 9.8m/s$^2$, 40kΩ | 50V, 24mW |
| Tian et al.(2022) [39] | Electromagnetic | 0.5Hz, 0.5m/s$^2$, 1kΩ | 3V, 5mW |
| | Piezoelectric | 0.5Hz, 0.5m/s$^2$, 6kΩ | 8V, 0.4mW |
| Zhang et al.(2017) [40] | Electromagnetic | 20Hz, 39.2m/s$^2$, 10kΩ | 2.4V, 3.7mW |
| | Piezoelectric | 20Hz, 39.2m/s$^2$, 1kΩ | 36V, 23mW |
| This work | Electromagnetic | 30Hz, 19.6m/s$^2$, 1.3kΩ | 16V, 20mW |
| | Piezoelectric | 30Hz, 19.6m/s$^2$, 19kΩ | 40V, 35mW |

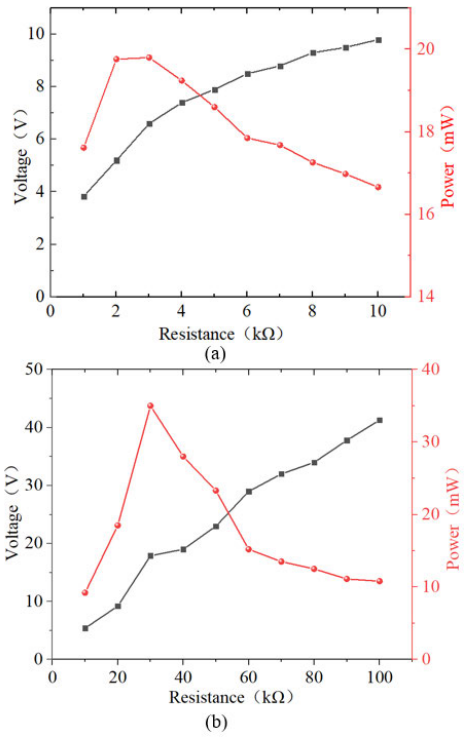


**FIGURE 8.** Peak voltage and peak power under different external loads. (a) EMG. (b) PEG.

using the hybrid harvester and the charging curves obtained are shown in Figure 9(e). The open circuit voltage curves after rectification under electromagnetic, piezoelectric and mixed conditions involved here are shown in supplementary material Figure S2.

To provide further verification of the prospects for use of energy harvesters in mechanical devices, tests were also conducted on a car engine as shown in Figure 10(a). Before the test, the acceleration spectrum of the automobile engine was tested using an acceleration sensor. Corresponding power spectral density curve was obtained through a MATLAB analysis and is shown in Figure 10(b). The figure shows that the car engine offers a better power output at around 30 Hz. The power harvester was placed in several positions around the engine to find the best working position. After testing, the energy harvester was placed at 45° above the engine and leaning against the back of the box to generate the best results. Connection to the rectifier bridge circuit allowed the thermometer to work properly, as illustrated in Figure 10(c). In addition, in order to verify the stability of the device, the hybrid energy harvester was operated for 1 hour every day for 30 days, and the measured output voltage could be well kept stable. The peak open-circuit voltage for 30 days is shown in supplementary material Figure S3.

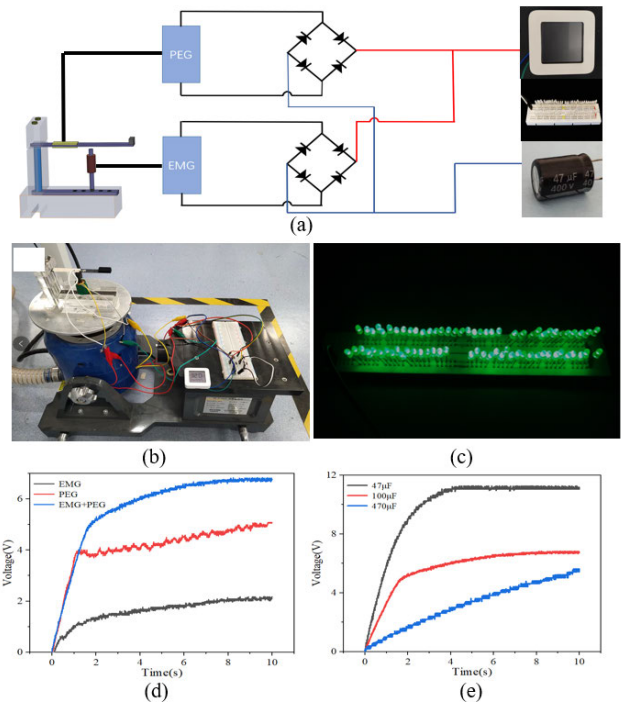


**FIGURE 9.** Energy harvester application testing in the laboratory. (a) Rectifier circuit and the test device. (b) Test scenario for powering a thermometer. (c) 50 LED lights are lit by the energy harvester. (d), (e) Capacitance charge test results.

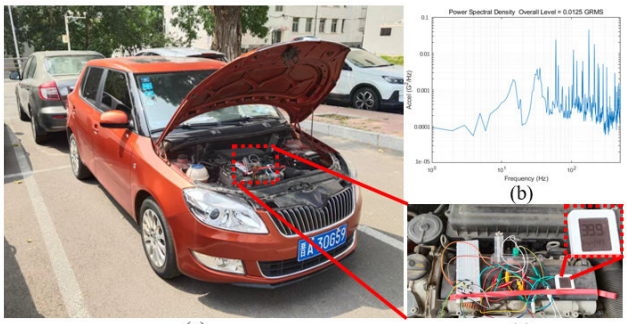


**FIGURE 10.** Application testing of Energy Harvester on a car engine. (a) Overall test scenario. (b) Power spectral density curve. (c) A thermometer powered by energy harvester.

## IV. CONCLUSION

In summary, to power sensor nodes for operation in critical parts of equipment in an industrial vibration environment, a method in which a magnetic circuit switch is applied to a hybrid electromagnetic–piezoelectric energy harvester is proposed. The main feature of this hybrid energy harvester is that the electromagnetic energy harvesting is performed by using vibrations to vary the gap between the cantilever beam and the coil column. Combination of this arrangement with a piezoelectric energy harvester on the cantilever beam provides further improvements in the power generation efficiency of the proposed hybrid energy harvester. In this paper, the feasibility of this hybrid harvester is illustrated using a combination of simulations and theoretical analysis, and a prototype device was trial-produced based on the proposed principle. Three different energy harvester modes were analysed and the parameters that affected the output voltage were tested to obtain the best output. The effect of application of the hybrid energy harvester was verified by performing laboratory application tests and automotive vibration environment tests. These verification tests showed that the hybrid energy harvester proposed in this paper provides a new method for the vibration energy harvesting field and that it has wide application prospects for use in industrial production.

## REFERENCES

[1] M. Shirvanimoghaddam, K. Shirvanimoghaddam, M. M. Abolhasani, M. Farhangi, V. Z. Barsari, H. Liu, M. Dohler, and M. Naebe, "Towards a green and self-powered Internet of Things using piezoelectric energy harvesting," *IEEE Access*, vol. 7, pp. 94533–94556, 2019.

[2] I. Ahmad, M. M. U. Rehman, M. Khan, A. Abbas, S. Ishfaq, and S. Malik, "Flow-based electromagnetic-type energy harvester using microplanar coil for IoT sensors application," *Int. J. Energy Res.*, vol. 43, no. 10, pp. 5384–5391, Aug. 2019.

[3] F. Kong, S. Yin, C. Sun, C. Yang, H. Chen, and H. Liu, "Design and optimization of a maglev electromagnetic–triboelectric hybrid energy converter for supplying power to intelligent sensing equipment," *Sustain. Energy Fuels*, vol. 6, no. 3, pp. 800–814, 2022.

[4] C. Lethien, J. Le Bideau, and T. Brousse, "Challenges and prospects of 3D micro-supercapacitors for powering the Internet of Things," *Energy Environ. Sci.*, vol. 12, no. 1, pp. 96–115, 2019.

[5] C. Jiang, X. Li, S. W. M. Lian, Y. Ying, J. S. Ho, and J. Ping, "Wireless technologies for energy harvesting and transmission for ambient self-powered systems," *ACS Nano*, vol. 15, no. 6, pp. 9328–9354, Jun. 2021.

[6] S. Zhang and X. Liao, "Research on micro-electro-mechanical system-based integrated energy harvester with test structures," *Energy Technol.*, vol. 9, no. 10, Oct. 2021, Art. no. 2100488.

[7] L. Hou, S. Tan, Z. Zhang, and N. W. Bergmann, "Thermal energy harvesting WSNs node for temperature monitoring in IIoT," *IEEE Access*, vol. 6, pp. 35243–35249, 2018.

[8] M. S. Kwak, M. Peddigari, Y. Min, J.-J. Choi, J.-H. Kim, M. A. Listyawan, J. Ryu, G.-T. Hwang, W.-H. Yoon, and J. Jang, "Boosting the lifespan of magneto-mechano-electric generator via vertical installation for sustainable powering of Internet of Things sensor," *Nano Energy*, vol. 101, Oct. 2022, Art. no. 107567.

[9] H. Lou, T. Wang, and S. Zhu, "Design, modeling and experiments of a novel biaxial-pendulum vibration energy harvester," *Energy*, vol. 254, Sep. 2022, Art. no. 124431.

[10] M. Iqbal and F. U. Khan, "Hybrid vibration and wind energy harvesting using combined piezoelectric and electromagnetic conversion for bridge health monitoring applications," *Energy Convers. Manage.*, vol. 172, pp. 611–618, Sep. 2018.

[11] M. A. Halim, R. Rantz, Q. Zhang, L. Gu, K. Yang, and S. Roundy, "An electromagnetic rotational energy harvester using sprung eccentric rotor, driven by pseudo-walking motion," *Appl. Energy*, vol. 217, pp. 66–74, May 2018.

[12] D. Castagnetti, "A Belleville-spring-based electromagnetic energy harvester," *Smart Mater. Struct.*, vol. 24, no. 9, Sep. 2015, Art. no. 094009.

[13] D. Castagnetti, "A simply tunable electromagnetic pendulum energy harvester," *Meccanica*, vol. 54, no. 6, pp. 749–760, Apr. 2019.

[14] S. Wang, G. Miao, S. Zhou, Z. Yang, and D. Yurchenko, "A novel electromagnetic energy harvester based on the bending of the sole," *Appl. Energy*, vol. 314, May 2022, Art. no. 119000.

[15] D. Castagnetti and F. Dallari, "Design and experimental assessment of an electromagnetic energy harvester based on slotted disc springs," *Proc. Inst. Mech. Eng., L, J. Mater., Des. Appl.*, vol. 231, nos. 1–2, pp. 89–99, Feb. 2017.

[16] C. Wang, Q. Zhang, W. Wang, and J. Feng, "A low-frequency, wideband quad-stable energy harvester using combined nonlinearity and frequency up-conversion by cantilever-surface contact," *Mech. Syst. Signal Process.*, vol. 112, pp. 305–318, Nov. 2018.

[17] A. R. Reddy, M. Umapathy, D. Ezhilarasi, and U. Gandhi, "Improved energy harvesting from vibration by introducing cavity in a cantilever beam," *J. Vib. Control*, vol. 22, no. 13, pp. 3057–3066, Jul. 2016.

[18] D. Liu, M. Al-Haik, M. Zakaria, and M. R. Hajj, "Piezoelectric energy harvesting using L-shaped structures," *J. Intell. Mater. Syst. Struct.*, vol. 29, no. 6, pp. 1206–1215, Apr. 2018.

[19] M. Fang, Q. Liao, J. Wang, L. Qin, C. Zhong, and D. Zhang, "Self-adaptive piezoelectric ceramic vibration system based on asymmetric piezoelectric cantilever for energy harvesting," *Int. J. Appl. Ceram. Technol.*, vol. 15, no. 5, pp. 1268–1276, Sep. 2018.

[20] D. Zou, G. Liu, Z. Rao, T. Tan, W. Zhang, and W.-H. Liao, "Design of a multi-stable piezoelectric energy harvester with programmable equilibrium point configurations," *Appl. Energy*, vol. 302, Nov. 2021, Art. no. 117585.

[21] M. Peddigari, M. S. Kwak, Y. Min, C.-W. Ahn, J.-J. Choi, B. D. Hahn, C. Choi, G.-T. Hwang, W.-H. Yoon, and J. Jang, "Lifetime estimation of single crystal macro-fiber composite-based piezoelectric energy harvesters using accelerated life testing," *Nano Energy*, vol. 88, Oct. 2021, Art. no. 106279.

[22] M. Feng, Y. Wu, Y. Feng, Y. Dong, Y. Liu, J. Peng, N. Wang, S. Xu, and D. Wang, "Highly wearable, machine-washable, and self-cleaning fabric-based triboelectric nanogenerator for wireless drowning sensors," *Nano Energy*, vol. 93, Mar. 2022, Art. no. 106835.

[23] Y. Han, W. Wang, J. Zou, Z. Li, X. Cao, and S. Xu, "Self-powered energy conversion and energy storage system based on triboelectric nanogenerator," *Nano Energy*, vol. 76, Oct. 2020, Art. no. 105008.

[24] C. Hou, T. Chen, Y. Li, M. Huang, Q. Shi, H. Liu, L. Sun, and C. Lee, "A rotational pendulum based electromagnetic/triboelectric hybrid-generator for ultra-low-frequency vibrations aiming at human motion and blue energy applications," *Nano Energy*, vol. 63, Sep. 2019, Art. no. 103871.

[25] L. Fang, Q. Zheng, W. Hou, L. Zheng, and H. Li, "A self-powered vibration sensor based on the coupling of triboelectric nanogenerator and electromagnetic generator," *Nano Energy*, vol. 97, Jun. 2022, Art. no. 107164.

[26] B. Zhao, Z. Li, X. Liao, L. Qiao, Y. Li, S. Dong, Z. Zhang, and B. Zhang, "A heaving point absorber-based ocean wave energy convertor hybridizing a multilayered soft-brush cylindrical triboelectric generator and an electromagnetic generator," *Nano Energy*, vol. 89, Nov. 2021, Art. no. 106381.
[27] Y. Li, Q. Guo, M. Huang, X. Ma, Z. Chen, H. Liu, and L. Sun, "Study of an electromagnetic ocean wave energy harvester driven by an efficient swing body toward the self-powered ocean buoy application," *IEEE Access*, vol. 7, pp. 129758–129769, 2019.
[28] X. Yang, C. Wang, and S. K. Lai, "A magnetic levitation-based tristable hybrid energy harvester for scavenging energy from low-frequency structural vibration," *Eng. Struct.*, vol. 221, Oct. 2020, Art. no. 110789.
[29] Z. Zhang, J. He, T. Wen, C. Zhai, J. Han, J. Mu, W. Jia, B. Zhang, W. Zhang, X. Chou, and C. Xue, "Magnetically levitated-triboelectric nanogenerator as a self-powered vibration monitoring sensor," *Nano Energy*, vol. 33, pp. 88–97, Mar. 2017.
[30] M. Iqbal, M. M. Nauman, F. U. Khan, P. E. Abas, Q. Cheok, A. Iqbal, and B. Aissa, "Multimodal hybrid piezoelectric-electromagnetic insole energy harvester using PVDF generators," *Electronics*, vol. 9, no. 4, p. 635, Apr. 2020.
[31] T. Wang, H. Lou, and S. Zhu, "Bandwidth enhancement of a gimbaled-pendulum vibration energy harvester using spatial multi-stable mechanism," *Appl. Energy*, vol. 326, Nov. 2022, Art. no. 120047.
[32] Y. Gu, W. Liu, C. Zhao, and P. Wang, "A goblet-like non-linear electromagnetic generator for planar multi-directional vibration energy harvesting," *Appl. Energy*, vol. 266, May 2020, Art. no. 114846.
[33] H.-X. Zou, M. Li, L.-C. Zhao, Q.-H. Gao, K.-X. Wei, L. Zuo, F. Qian, and W.-M. Zhang, "A magnetically coupled bistable piezoelectric harvester for underwater energy harvesting," *Energy*, vol. 217, Feb. 2021, Art. no. 119429.
[34] S. G. Burrow, L. R. Clare, A. Carrella, and D. Barton, "Vibration energy harvesters with non-linear compliance," in *Active and Passive Smart Structures and Integrated Systems 2008*. 2008.
[35] A. R. M. Siddique, S. Mahmud, and B. Van Heyst, "Energy conversion by 'T-shaped' cantilever type electromagnetic vibration based micro power generator from low frequency vibration sources," *Energy Convers. Manage.*, vol. 133, pp. 399–410, Feb. 2017.
[36] D. Zhao, S. Liu, Q. Xu, W. Sun, T. Wang, and Q. Cheng, "Theoretical modeling and analysis of a 2-degree-of-freedom hybrid piezoelectric–electromagnetic vibration energy harvester with a driven beam," *J. Intell. Mater. Syst. Struct.*, vol. 29, no. 11, pp. 2465–2476, Jul. 2018.
[37] J. Zhou, L. He, L. Liu, G. Yu, X. Gu, and G. Cheng, "Design and research of hybrid piezoelectric-electromagnetic energy harvester based on magnetic couple suction-repulsion motion and centrifugal action," *Energy Convers. Manage.*, vol. 258, Apr. 2022, Art. no. 115504.
[38] C. Wang, S.-K. Lai, Z.-C. Wang, J.-M. Wang, W. Yang, and Y.-Q. Ni, "A low-frequency, broadband and tri-hybrid energy harvester with septuple-stable nonlinearity-enhanced mechanical frequency up-conversion mechanism for powering portable electronics," *Nano Energy*, vol. 64, Oct. 2019, Art. no. 103943.
[39] S. Tian, X. Wei, L. Lai, B. Li, Z. Wu, and Y. Dai, "Frequency modulated hybrid nanogenerator for efficient water wave energy harvesting," *Nano Energy*, vol. 102, Nov. 2022, Art. no. 107669.
[40] Z. Zhang, J. He, J. Han, H. Xu, J. Mu, T. Wen, D. Wang, Z. Tian, Z. Chen, and C. Xue, "Magnetically levitated/piezoelectric/triboelectric hybrid generator as a power supply for the temperature sensor," *Sci. China Technol. Sci.*, vol. 60, no. 7, pp. 1068–1074, Jul. 2017.

**XIANG GAO** was born in Shanxi, China, in 1986. He received the M.S. degree in control science and engineering from the Taiyuan University of Technology, in 2013. He is currently pursuing the Ph.D. degree with the Key Laboratory of Instrumentation Science and Dynamic Measurement, Ministry of Education, North University of China. His research interest includes micro-energy conversion and management.

**JUAN CUI** received the Ph.D. degree in mechanical engineering from the Beijing Institute of Technology, Beijing, China, in 2020. Since 2020, she has been an Associate Professor with the North University of China. Her research interests include high-performance triboelectric nanogenerator and micro energy systems.

**YONGQIU ZHENG** received the Ph.D. degree in test and measurement technology and instrumentation from the North University of China, in 2015. He is mainly engaged in research on high-temperature and high-pressure optical MEMS sensor devices, high-Q micro-cavity sensing testing, and complex environment vibration micro-energy harvesting and application. He has presided over one project of the National Key Research and Development Program of Ministry of Science and Technology, one project of the National Natural Science Foundation of China, and two projects of the Department of Equipment Development Field Fund of Military Commission.

**GANG LI** received the B.S. degree in automation from the Hebei University of Science and Technology, in 2020. He is currently pursuing the master's degree with the Key Laboratory of Instrumentation Science and Dynamic Measurement, Ministry of Education, North University of China. His research interest includes micro-energy conversion and management.

**CONGCONG HAO** received the B.S. and M.S. degrees from the North University of China, Taiyuan, China, and the Ph.D. degree from the Science and Technology on Electronic Test and Measurement Laboratory, North University of China. Since 2022, she has been a Lecturer with the North University of China. Her main research interest includes energy harvesting.

**CHENYANG XUE** received the B.S. degree in theoretical physics from the Department of Physics, Shanxi University, in 1994, the M.S. degree in quantum optics and laser technology from the Institute of Optoelectronics, Shanxi University, in 1997, and the Ph.D. degree in semiconductor materials from the Department of Physics, Athens University of Science and Technology, Greece, in 2003. He is engaged in the research of micro and nano sensing and testing technology, presiding over 863 projects, National Defense 973 projects, and basic scientific research of National Defense Science and Industry Commission.